Inhibition of Immunoglobulin E Attenuates Pulmonary Hypertension

Shu Ting
  State Key Laboratory of Medical Molecular Biology, Institute of Basic Medical Sciences, Chinese Academy of Medical Sciences

Liu Ying
  State Key Laboratory of Medical Molecular Biology, Institute of Basic Medical Sciences, Chinese Academy of Medical Sciences

Zhou Yitian
  Peking Union Medical College, MD Program

Zhou Zhou
  Fuwai Hospital

Yang Peiran
  Institute of Basic Medical Sciences, Chinese Academy of Medical Sciences

Li Jinqiu
  Institute of Basic Medical Sciences, Chinese Academy of Medical Sciences

Xing Yanjiang
  Institute of Basic Medical Sciences, Chinese Academy of Medical Sciences

Song Xiaomin
  Institute of Basic Medical Sciences, Chinese Academy of Medical Sciences

Li Bolun
  Institute of Basic Medical Sciences, Chinese Academy of Medical Sciences

Pang Junling
  Institute of Basic Medical Sciences, Chinese Academy of Medical Sciences

Ning Xin
  Institute of Basic Medical Sciences, Chinese Academy of Medical Sciences

Qi Xianmei
  Institute of Basic Medical Sciences, Chinese Academy of Medical Sciences

Xiong Changming
  Fuwai Hospital

Yang Hang
  Fuwai Hospital

Chen Qianlong
  Fuwai Hospital

Chen Jingyu

The Affiliated Wuxi People's Hospital of Nanjing Medical University

Yu Ying

Tianjin Medical University

Wang Jing (✉ wangjing@ibms.pumc.edu.cn)

State Key Laboratory of Medical Molecular Biology, Institute of Basic Medical Sciences, Chinese Academy of Medical Sciences

Wang Chen

Chinese Academy of Medical Sciences

Article

Abstract

Pulmonary hypertension (PH) is a severe cardiopulmonary disease characterized by pathological vascular remodeling in the lung. Immunoglobulin E (IgE) is known to participate in aortic vascular remodeling, but whether IgE mediates pulmonary vascular remodeling in PH is unknown. Here, we found serum IgE elevation in PAH patients, hypoxia-induced PH mice and monocrotaline (MCT)-induced PH rats. Combining animal model of PH with single-cell RNA sequencing, we found IgE production in the lung tissues of PH mice. Neutralizing IgE with an anti-IgE antibody was effective in preventing PH development in mice and rat models. The IgE receptor FcεRIα was also upregulated in PH lung tissues and Fcer1a deficiency prevented the development of PH in mice. Single-cell RNA-seq revealed that FcεRIα was mostly expressed in mast cells, and mast cell-specific Fcer1a knockout protected against PH in mice. Further mechanistic experiments revealed that IgE-activated mast cells produced interleukins IL6 and IL13, which subsequently promoted vascular muscularization. Clinically approved IgE antibody Omalizumab alleviated the progression of established PH in rats. Using genetic and pharmacological approaches, we have demonstrated that blocking IgE- FcεRIα signaling may hold potential for the treatment of PAH.

1 Introduction

Pulmonary hypertension (PH) is a progressive cardiopulmonary disease that results in increased mean pulmonary arterial pressure (mPAP), ultimately leading to failure of the right ventricle and death. Pulmonary vascular remodeling and infiltration of immune cells are important pathological features in pulmonary arterial hypertension (PAH, WHO Group 1) [1, 2]. Chronic inflammation is observed in lung tissues from experimental PH models and PAH patients. Immune cells and pro-inflammatory factors are thought to contribute to vascular remodeling and muscularization. Of note, lymphoid follicles are found in hypoxia-exposed animals and contain T cells, B cells and dendritic cells [3, 4]. Moreover, IPAH patients without auto-immune diseases also produce auto-antibodies [5-7], suggesting that the adaptive immune response occurs locally to generate antibodies in the lung. Currently available therapies for PAH are unable to reverse the pathological vascular remodeling and do not target the dysregulated immune response in the vessel wall. Elucidating the mechanism of vascular remodeling and inflammation may facilitate the identification of novel and more effective therapeutic targets.

Immunoglobulin E (IgE) is an antibody secreted by B cells that undergo IgE class-switch recombination and up-regulate germ-line ε (*Glε*) transcription [8] in response to Th2 stimulation. B cells and tertiary lymphoid organs are found in arterial wall lesions in atherosclerosis [9]. We previously reported that serum IgE is elevated during the aortic vascular remodeling in cardiovascular diseases such as atherosclerosis [10] and abdominal aortic aneurysm [11]. IgE aggravates perivascular inflammation by binding to FcεRIα, the α-subunit of its high affinity receptor [12]. Mast cells (MCs) and other cell types play a major role in cardiovascular diseases mediated by high serum IgE levels [10]. Moreover, MC infiltration has been identified in the lung tissues from patients with idiopathic PAH (IPAH) and rats with monocrotaline (MCT)-induced PH [13, 14], while inhibition of MCs by cromolyn, an MC stabilizer,

repressed the development of PH in rats [13]. However, the roles of IgE in PH development and the cell types mediating its effects are not known, and whether this effect is amenable to therapeutic targeting remains unclear.

In this study, we identified increased serum IgE levels in clinic IPAH patients and experimental PH models. We showed that blocking IgE effectively prevented PH in multiple animal models. We demonstrated that IgE promoted vascular muscularization by binding with FcεRIα, activating MCs and promoting the release of IL6 and IL13. The clinically used anti-IgE antibody Omalizumab showed therapeutic effect in rats with established PH.

2 Materials And Methods

2.1 PAH and control Subjects

A total of 124 patients with idiopathic or heritable PAH and 116 age- and sex-matched non-PAH subjects were enrolled in a single-center clinical cohort from 2016-2018 in Fuwai Hospital. For patients, the diagnosis of IPAH/HPAH was based on the 2015 ESC/ERS guidelines, and was confirmed to meet the new criteria defined in the 6th World Symposium on Pulmonary Hypertension, 2018. Subjects with (1) allergy, infection or autoimmune diseases; (2) tumors or fibrosis; and (3) juvenile age under 18 were excluded. Control subjects were recruited from a pool of healthy volunteers at Fuwai Hospital. A health questionnaire that included medical history and medication history was used to screen potential participants. Age/sex-matched individuals without pulmonary hypertension, cardiovascular diseases, pulmonary diseases, cancer, infection, allergy, or autoimmune diseases were included. Individuals with abnormal BMI and abnormal routine blood indices were excluded. Four PAH lung tissues were obtained from the China-Japan Friendship Hospital Lung Transplantation Center during 2018-2019. Specimens that had (1) lung infection, (2) allergic diseases, autoimmune diseases or (3) complicated pulmonary diseases (tumor, fibrosis, etc.) were excluded. Four non-PAH lung tissue samples were collected from healthy transplant donors. All studies in this report were first approved by the Institutional Ethics Committee of Peking Union Medical College (2018043) and Fuwai Hospital (Approval NO. 2017-877). Informed consents to use lung tissue for research were provided by PAH participants before enrollment.

2.2 Animal experiments

For rodent models of PH, mice with chronic hypoxia-induced PH (10-week old, 10% O_2, 4 weeks) and rats monocrotaline (MCT)-induced PH (200 g, 60mg/kg MCT, one injection, 4 weeks) were used. For pharmacological studies, hypoxic mice were treated with anti-IgE antibody (553416, BD) or isotype control antibody (555839, BD), monocrotaline-injected rats were treated with anti-IgE antibody (553914, BD), isotype control antibody (554121, BD), or Omalizumab (Novartis). For genetic studies, $Fcer1a^{-/-}$ (knockout, KO) mice (background C57BL/6) were purchased from the Jackson Laboratory (Bar Harbor, ME). C57BL/6 (wildtype, WT) mice were purchased from Beijing Vital River Laboratory Animal Technology Co., Ltd. $Fcer1a$ flox/flox (Biocytogen) and $Mcpt5$-Cre mice (Biocytogen) were crossbred to

generate $Fcer1a^{flox/flox}$-$Mcpt5^{Cre/+}$ and $Fcer1a^{flox/flox}$-$Mcpt5^{+/+}$ mice. Animals were randomly divided into the different groups for each experiment. All animal experiments were conducted under protocols approved by the Animal Research Committee of the Institute of Laboratory Animals, Chinese Academy of Medical Sciences and Peking Union Medical College (ACUC-A01-2018-005). Further details of the animal experiments and analyses are available in the supplementary material.

2.3 Single-cell RNA-seq and analysis

Lung tissues from mice under hypoxia exposure for 0, 1, 2 and 4 weeks were harvested and scRNA-seq were performed. A single-cell cDNA library was generated as previously described [15]. More details of the analysis are available in the supplementary material.

2.4 Statistical analyses

All statistical analyses were performed using GraphPad Prism 8.0 and SPSS version 23.0. Data are presented as means ± standard error of mean (SEM). The Kolmogorov-Smirnov test was used to assess for normality. An unpaired two-tailed t-test was performed to compare the difference between two groups. A one-way ANOVA with LSD-t test or two-way ANOVA with Bonferroni's post hoc test was performed to evaluate differences between multiple groups. A p-value <0.05 was considered statistically significant. Randomization and blinded analyses were used whenever possible.

2.5 Additional materials and methods

Additional materials and methods are available in the supplementary material online.

3 Results And Discussion

3.1 Elevated serum IgE in PAH patients and PH models

We examined IPAH/HPAH patients who did not have allergy, infection or autoimmune diseases (**Supplementary Table 1**), and found that these PAH patients showed elevated serum IgE levels in comparison with age/sex-matched healthy subjects (**Fig.1A**). In experimental PH models, elevated serum IgE levels were observed in hypoxia-induced PH mice (**Fig.1B**) and MCT-induced PH rats (**Fig.1C**) when compared with control animals.

Adaptive immune response is observed in PH lung[16], therefore we hypothesized that the elevated IgE is produced from lung tissues. To characterize the local immune response in lung tissues and the cells involved, single cell RNA sequencing (scRNA-seq) was performed in lung tissues from mice exposed to hypoxia at different time points (**Supplementary Fig.1**). The proportion of B cells (identified by their characteristic enrichment of *Cd19*, **Fig.1D and E**) was increased under hypoxia (**Fig.1F**). Differentially expressed genes (DEGs, **Fig.1G**) and their enriched Gene Ontology (GO) terms between consecutive pairs of time points revealed "B cell activation" and "B cell differentiation" at the early stages of PH (**Supplementary Fig.2**). GO terms of "regulation of chromosome organization", "regulation of

immunoglobin mediated immune response", and "immunoglobulin mediated immune response" (**Supplementary Fig.2**) suggested that antibody class-switch recombination may have occurred in B cells during PH development. We also found enhanced Th2 response (**Supplementary Fig.3A-D**), up-regulated transcription of genes in the IL4 pathway in T cells (**Supplementary Fig.3E**), as well as enhanced $Cd4^+$ T-B cell interactions (**Supplementary Fig.3F-H**), supporting that IgE was produced by activated B cells in PH lung via a classical mechanism. These results were experimentally confirmed by the increased proportion of activated B cells ($CD21^+CD23^+$) in hypoxic lung (**Fig.1H**). Moreover, the upregulation of $Gl\varepsilon$ mRNA expression in both $CD19^+$ B cells and PH lung tissues (**Fig.1I**) further confirmed that active B cells switched to the IgE isotype. The increased percentage of IgE^+ cells in PH lungs (**Fig.1J**) potentially resulted in the elevation of serum IgE levels during PH development.

3.2 Blocking serum IgE attenuated the development of PH in mice and rats

To determine the function of IgE in PH development, we used an experimental anti-IgE antibody to neutralize serum IgE in a hypoxic mouse model of PH (**Fig.2A, Supplementary Fig.4A**). In mice exposed to hypoxia, the anti-IgE antibody significantly attenuated the increase in right ventricular systolic pressure (RVSP, **Fig.2B**), reduced the extent of right ventricular hypertrophy (RV/LV+S, **Fig.2C**), and restored the ratio of pulmonary artery acceleration time over ejection time (PA AT/ET, **Fig.2D**), compared with hypoxic mice administered with the isotype control antibody. Moreover, the anti-IgE antibody also attenuated hypoxia-induced pulmonary vascular muscularization, as indicated by the decreased pulmonary vascular wall thickness (**Fig.2E and F**), increased percentage of non-muscularized vessels (N), and decreased percentage of fully muscularized vessels (F) compared to the isotype antibody-treated animals (**Fig.2G**).

We further confirmed the role of IgE in rats with MCT-induced PH (**Fig.2H, Supplementary Fig.4B**). The results showed that MCT-injected rats treated with the anti-IgE antibody exhibited significantly reduced mPAP (**Fig.2I**), reduced right ventricular hypertrophy (**Fig.2J**) and improved PA AT/ET (**Fig.2K**) compared those administered with the isotype control. The anti-IgE antibody also decreased pulmonary vascular wall thickness (**Fig.2L and M**) and attenuated vascular muscularization (**Fig.2N**) caused by MCT. Taken together, these results indicate that blocking serum IgE conferred protection against experimental PH.

3.3 *Fcer1a* deficiency attenuated hypoxia-induced PH in mice

To identify the target receptor for IgE in PH development, we assessed the expression of the high affinity receptor FcεRIα in the lung tissues from PAH patients. We observed that FcεRIα mRNA and protein levels were significantly up-regulated in the patient lung (**Fig.3A and B**). Immunohistochemical staining showed that FcεRIα positive cells were located around pulmonary vessels (**Fig.3C**), suggesting their potential involvement in pulmonary vascular remodeling. In lung tissues from hypoxia-exposed mice (**Fig.3D and E**) and MCT-injected rats (**Fig.3F and G**), mRNA and protein levels of FcεRIα were also increased. To investigate the role of FcεRIα in IgE-mediated PH, $Fcer1a^{+/+}$ (WT) and $Fcer1a^{-/-}$ (KO) mice were exposed to hypoxia to establish PH (**Fig.3H**). As shown in **Fig.3I-K**, *Fcer1a* deficiency protected against hypoxia-induced elevation in RVSP and RV hypertrophy, and decrease in PA AT/ET compared with WT mice.

Histological analyses showed less pulmonary vascular thickening and muscularization in response to hypoxia in *Fcer1a* knockout mice compared to WT controls (**Fig.3L-N**). These results indicated that FcεRIα was the receptor involved in IgE-mediated PH development.

3.4 FcεRIα expressed in mast cells contributed to PH development in mice

To identify the FcεRIα expressing cells in lung tissues, we analyzed our mouse scRNA-seq data and found that *Fcer1a* was mainly enriched in MCs (**Fig.4A, top**). Similarly, the published scRNA-seq data [17] in normal human lungs revealed *FCER1A* expression in MCs (**Fig.4A, bottom**). These results were confirmed by the co-localization of FcεRIα$^+$ cells and MC markers (c-Kit$^+$ cells, **Fig.4B**). Moreover, we showed an increased percentage of CD45$^+$ c-Kit$^+$ FcεRIα$^+$ cells (MCs) in hypoxic mice (**Fig.4C**). This observation is consistent with the previous report of MCs infiltration in lung tissues of PAH patients and PH rats[18].

To evaluate the function of MC-expressed FcεRIα in PH development, MC-specific *Fcer1a* knockout mice (*Fcer1a*$^{MC-/-}$, MCKO) were generated by crossbreeding *Fcer1a*$^{flox/flox}$ mice (WT) mice with *Mcpt5-Cre* transgenic mice (**Fig.4D**). Four weeks of hypoxia exposure resulted in PH in WT mice, indicated by increased RVSP and decreased PA AT/ET, which were improved in the MCKO mice (**Fig.4E and G**). No significant changes were observed in RV hypertrophy, consistent with previous findings of cromolyn administration in MCT model [13] (**Fig.4F**). Histological analyses showed decreased wall thickness and vascular muscularization in MCKO compared with WT mice under hypoxia (**Fig.4H-J**). Together, these results suggested that FcεRIα expressed in MCs contributed to the development of PH.

3.5 IgE stimulated MCs to produce IL6 and IL13 in experimental PH models

In order to identify the factors by which IgE-activated MCs mediate PH pathogenesis, MCs were treated with IgE to mimic their response to IgE in lung tissues, followed by RNA-seq to identify IgE-regulated genes. Previous studies indicated that the MCs were recruited from bone marrow to the lung in PH [14]; therefore, bone marrow derived mast cells (BMMCs) were used for this experiment. As shown in **Fig.5A**, IgE treatment altered the expression of 6,041 genes in BMMCs. GO analyses showed that the IgE-regulated genes were primarily associated with inflammation and vascular cell dysfunction (**Fig.5B**). Importantly, the DEGs enriched in these GO terms included many secreted factors that are known to be PH-related, such as *Il6*, *Il13*, *Il33*, *Vegfa*, *Vegfb*, *Vegfc*, *Fgf2*, *Fgf18*, *Hbegf*, *Pdgfa*, *Ccl2* and *Ccl4* (**Fig.5A**). By combining these 12 genes from the RNA-seq data of IgE-stimulated MCs with our scRNA-seq data from PH animals, we found three candidate genes (*Il6*, *Ccl4* and *Il13*) that were mainly expressed by MCs and responded to IgE stimulation (**Fig.5C**). RT-qPCR results confirmed the significantly up-regulated expression of *Il6* and *Il13*, but not *Ccl4*, in CD45$^+$ c-Kit$^+$ FcεRIα$^+$ MCs sorted from hypoxic lung tissues (**Fig.5D**). Moreover, increased *Il6* and *Il13* expression was observed in lung tissues from hypoxic mice (**Fig.5E**), and their expression was reduced under IgE-FcεRIα blockade, as shown in anti-IgE antibody-treated mice (**Fig.5F**), *Fcer1a* knockout mice (**Fig.5G**), as well as in MC-specific *Fcer1a* knockout mice (**Fig.5H**). Similarly, *Il6* and *Il13* expression was also increased in MCT-injected rats (**Supplementary**

Fig.5A), and was reduced by anti-IgE (**Supplementary Fig.5B**). Co-culture of MCs and PASMCs was established to study the effects of MC derived IL6 and IL13 (**Fig.5I**). The conditioned medium of IgE-activated MCs promoted PASMC proliferation, while this pro-proliferative effect of the conditioned medium was reduced with knockdown of *Il6* and *Il13* in MCs (**Fig.5J and K**). Through a series of transcriptomic analysis and experimental validation, we have found that IgE-activated MCs produced IL6 and IL13, which potentially contributed to IgE-mediated PH in animal models.

3.6 Clinically-used IgE antibody Omalizumab ameliorated established PH in rats

We next evaluated the effect of anti-IgE therapy on the progression of established PH in rats using Omalizumab, a clinically-used recombinant human monoclonal antibody. The treatment was started from 14 days post-MCT injection, when the pulmonary vascular remodeling and mPAP elevation were already present [19] (**Fig.6A**). After two weeks of treatment, Omalizumab effectively lowered the serum IgE levels (**Fig.6B**), reduced mPAP (**Fig.6C**) and RV hypertrophy (**Fig.6D**), improved pulmonary artery ejection function (**Fig.6E**), and attenuated pulmonary vascular wall thickening and muscularization (**Fig.6F-H**). Anti-IgE therapy by Omalizumab also decreased *Il6* and *Il13* expression effectively in lung tissues of MCT-induced PH rats (**Fig.6I**). These results indicate that Omalizumab attenuates the development of established PH, and targeting IgE may serve as an effective therapy for PH patients especially with high serum IgE.

4 Discussion

In this study, we have discovered that IgE was elevated in PAH patients and animal models of PH, and this promoted the pathogenesis of disease. We have shown that blocking IgE effectively attenuated the development of PH in different models. Using constitutive and cell type-specific knockout animals, IgE was found to promote PH by stimulating MCs to produce IL6 and IL13, revealing a novel immune-based mechanism in PH (**Supplementary Fig.6**). This is the first report of the function of IgE in pulmonary vascular disease. Our findings provide pre-clinical evidence supporting the translation of anti-IgE therapies such as Omalizumab in the treatment of PAH.

Elevation of IgE is well recognized to be important in cardiovascular diseases. Our study showed that IgE was also elevated in PH, released from stimulated B cells in lung tissues. Previous studies have reported that auto-antigen exposure in pulmonary arterial vessels could activate the immune system in PH lung tissues [5, 7]. These auto-antigens, including lamin A/C, tubulin β-chain in endothelial cells, as well as vimentin and calumenin in fibroblasts, triggered the production and binding of IgG/IgM isotype antibody. Moreover, infiltration of Th2 cells and production of Th2 cytokines (IL4, IL5, IL13) have been reported in lung tissues from PAH patients or PH animal models [20, 21]. In this study, we first revealed increased Th2 cell-B cell interaction in the lung tissues of PH mice through scRNA-seq. This process may promote antibody class switching into the IgE isotype in B cells, subsequently leading to increased IgE production. Collectively, we propose that the exposure of auto-antigens in damaged pulmonary vessels elicits a local adaptive immune response, resulting in IgE production during PH development.

Exogenous antigens such as mite or pollen may also cause IgE elevation, in the context of asthma or allergic reaction. However, there is no confirmed clinical relationship between asthma and PH. IgE is not necessary for all types of asthma, as IgE elevation and reactivity are not observed in patients with IgE-independent asthma [22]. Besides, The IgE level has an aggravated elevation in patients with asthma at acute attack, which gets back to normal level when patient is recovered [23]. More importantly, IgE derived from exogenous antigens shows component-specificity. Component-specific IgE may exhibit different disease-causing effects, as illustrated in other types of cardiovascular diseases [24]. In our study, we did not use PH models caused by dust mites or ovalbumin, and the serum and tissue samples were collected from PAH patients without allergy, infection or autoimmune diseases. Hence, IgE was activated by endogenous auto-antigens and was functional in PH development. Transfusing purified IgE from PH rats into naïve rat could support the function of endogenous IgE in PH. This experiment is worthwhile further investigation once the purification technique is improved.

FcεRIα is the high affinity receptor that interacts with IgE directly. We observed increased FcεRIα expression in the lung tissues of rodent PH models and PAH patients. Perivascular FcεRIα⁺ cells were rare in the lung tissues of non-PAH subjects, which was consistent with a previous report [25]. Remarkably, in PAH lung tissues, we found significant increases in FcεRIα⁺ cells around the vascular lesions. The mechanism driving the increase in FcεRIα expression in PH lung is unclear. Importantly, scRNA-seq data of mice, rats and human lung tissues all revealed FcεRIα expression in MCs. Bone-marrow derived mast cells, which infiltrate into the lung tissue and constitute the perivascular MCs, possess high FcεRIα expression [26], but whether these infiltrated MCs contributed to elevating FcεRIα level warrants further investigation. Based on our results, a concomitant increase in IgE production and its effector cells with the high affinity receptor gives rise to a series of downstream responses that may ultimately result in vascular remodeling.

Activation of MCs has been reported in MCT-induced PH rat and human lung tissues from PAH patients [13, 14]. Stabilizing MCs through cromolyn in the early stage protects against MCT-induced PH development [13]. However, the mechanism by which MCs are activated remains unknown to date. Our results revealed that increased IgE in PH activated MCs and contributed to the development of PH. Among a range of MC-released downstream mediators, we narrowed down the predominant factors to IL6 and IL13 using transcriptomic and experimental approaches. IL6 is widely recognized to be important in PH, as circulating IL6 was elevated in patients with PAH [27, 28]. Moreover, IL6 was reported to be important for IgE generation from B cells, and MC-derived IL6 was shown to promote PH by stimulating B cells [29]. These results suggested that MC-derived IL6 may reciprocally activate B cells to secrete more IgE, forming a vicious cycle in disease pathogenesis. Additionally, IL13 may also participate in PH, as transgenic mice overexpressing IL13 in the lung spontaneously developed PH. IL13 was reported to promote the proliferation of pulmonary arterial smooth muscle cells [30] and migration of pulmonary arterial endothelial cells [31]. Taken together, we have shown that IgE served as an activator of MCs and the subsequent release of cytokines, in particular IL6/IL13, promoted pulmonary vascular remodeling.

Limitations of our study include the species difference in the expression of FcεRIα. In addition to MCs, FcεRIα is also expressed in dendritic cells in human (**Fig.4B**), whereas its expression is absent in murine counterparts [32]. Infiltration of dendritic cells was observed in human PAH lung samples [33]. Previous research has reported conflicting roles of FcεRIα expressed in dendritic cells, due to the different research strategies used [34, 35]. The observations in humanized mice [35] suggested that IgE activation mediated antigen presentation by dendritic cells. In the pathogenesis of asthma in human [22], IgE activated dendritic cells promoted Th2 cell recruitment and reactivation. Based on these reports and the expression of FcεRIα in human dendritic cells, we speculate that IgE may act on dendritic cells to promote the infiltration of Th2 cells, leading to an uncontrolled Th2 response in PH. Of note, stabilizing MCs by cromolyn is effective in treating PH in rats, but less effective in human [36]. This might be explained by the infiltrated dendritic cells in human lung, which are also activated by IgE but are unresponsive to cromolyn. From a translational perspective, blocking the upstream mediator IgE, instead of a single type of downstream effector cells (MCs or dendritic cells) and factors (IL6 or IL13), may confer better therapeutic efficacy. In order for this concept to be applied in the clinic, further pre-clinical and clinical studies are required, to compare the efficacy of Omalizumab, against and/or in combination with currently available drugs for PAH, in order to determine the most suitable IgE blocker for single or combination therapy. The wealth of data and experiences associated with the use of Omalizumab in other diseases may facilitate its repurposing for the treatment of PAH.

In summary, our study demonstrated that elevated IgE promoted the development of PH, whilst inhibition of IgE attenuated PH in multiple animal models. This pathogenic axis was shown to be activated in PAH patients. We have found that the IgE antagonist Omalizumab ameliorated established PH, providing proof-of-concept supporting this novel therapeutic strategy, especially for PAH patients with high levels of serum IgE.

Declarations

Author contributions

Ting Shu: Investigation, Methodology, Visualization, Writing - Original Draft

Ying Liu: Investigation, Methodology, Visualization, Formal analysis

Yitian Zhou: Investigation, Software, Formal analysis, Data Curation, Visualization

Zhou Zhou: Resources, Formal analysis, Project administration

Peiran Yang: Supervision, Writing - Review & Editing

Jinqiu Li: Investigation, Validation, Visualization

Yanjiang Xing: Investigation, Writing - Review & Editing

Xiaomin Song: Validation, Visualization

Bolun Li: Software, Data Curation

Junling Pang: Software, Data Curation

Xin Ning: Investigation, Validation

Xianmei Qi: Investigation, Validation

Changming Xiong: Resources, Formal analysis

Hang Yang: Resources

Qianlong Chen: Resources

Jingyu Chen: Supervision, Resources

Ying Yu: Supervision, Writing - Review & Editing

Jing Wang: Conceptualization, Supervision, Writing - Review & Editing, Project administration, Funding acquisition

Chen Wang: Conceptualization, Supervision, Writing - Review & Editing, Project administration, Funding acquisition

Conflict of interest: The authors declare that they have no conflict of interest.

References

1.   Sakao, S., N.F. Voelkel, and K. Tatsumi, *The vascular bed in COPD: pulmonary hypertension and pulmonary vascular alterations.* Eur Respir Rev, 2014. **23**(133): p. 350-5.

2.   Humbert, M., et al., *Pathology and pathobiology of pulmonary hypertension: state of the art and research perspectives.* Eur Respir J, 2019. **53**(1).

3.   Colvin, K.L., et al., *Bronchus-associated lymphoid tissue in pulmonary hypertension produces pathologic autoantibodies.* Am J Respir Crit Care Med, 2013. **188**(9): p. 1126-36.

4.   Frid, M.G., et al., *Immunoglobulin-driven Complement Activation Regulates Proinflammatory Remodeling in Pulmonary Hypertension.* Am J Respir Crit Care Med, 2020. **201**(2): p. 224-239.

5.   Terrier, B., et al., *Identification of target antigens of antifibroblast antibodies in pulmonary arterial hypertension.* Am J Respir Crit Care Med, 2008. **177**(10): p. 1128-34.

6.   Arends, S.J., et al., *Prevalence of anti-endothelial cell antibodies in idiopathic pulmonary arterial hypertension.* Eur Respir J, 2010. **35**(4): p. 923-5.

7.   Dib, H., et al., *Targets of anti-endothelial cell antibodies in pulmonary hypertension and scleroderma.* Eur Respir J, 2012. **39**(6): p. 1405-14.

8.   Kashiwada, M., et al., *IL-4-induced transcription factor NFIL3/E4BP4 controls IgE class switching.* Proc Natl Acad Sci U S A, 2010. **107**(2): p. 821-6.

9.   Srikakulapu, P., et al., *Artery tertiary lymphoid organs control multilayered territorialized atherosclerosis B-cell responses in aged ApoE-/- mice.* Arterioscler Thromb Vasc Biol, 2016. **36**(6): p. 1174-85.

10.   Wang, J., et al., *IgE stimulates human and mouse arterial cell apoptosis and cytokine expression and promotes atherogenesis in Apoe-/- mice.* J Clin Invest, 2011. **121**(9): p. 3564-77.

11.   Wang, J., et al., *IgE actions on CD4+ T cells, mast cells, and macrophages participate in the pathogenesis of experimental abdominal aortic aneurysms.* EMBO Mol Med, 2014. **6**(7): p. 952-69.

12.   Wu, L.C. and A.A. Zarrin, *The production and regulation of IgE by the immune system.* Nat Rev Immunol, 2014. **14**(4): p. 247-59.

13.   Bartelds, B., et al., *Mast cell inhibition improves pulmonary vascular remodeling in pulmonary hypertension.* Chest, 2012. **141**(3): p. 651-660.

14.   Montani, D., et al., *C-kit-positive cells accumulate in remodeled vessels of idiopathic pulmonary arterial hypertension.* Am J Respir Crit Care Med, 2011. **184**(1): p. 116-23.

15.   Xie, T., et al., *Single-Cell Deconvolution of Fibroblast Heterogeneity in Mouse Pulmonary Fibrosis.* Cell Rep, 2018. **22**(13): p. 3625-3640.

16.   Shu, T., Y. Xing, and J. Wang, *Autoimmunity in Pulmonary Arterial Hypertension: Evidence for Local Immunoglobulin Production.* Frontiers in Cardiovascular Medicine, 2021. **8**(1056).

17.   Travaglini, K.J., et al., *A molecular cell atlas of the human lung from single-cell RNA sequencing.* Nature, 2020. **587**(7835): p. 619-625.

18.   Dahal, B.K., et al., *Involvement of mast cells in monocrotaline-induced pulmonary hypertension in rats.* Respir Res, 2011. **12**: p. 60.

19.   Huang, J., et al., *Progressive endothelial cell damage in an inflammatory model of pulmonary hypertension.* Exp Lung Res, 2010. **36**(1): p. 57-66.

20.   Daley, E., et al., *Pulmonary arterial remodeling induced by a Th2 immune response.* J Exp Med, 2008. **205**(2): p. 361-72.

21.   Chen, G., et al., *Inhibition of CRTH2-mediated Th2 activation attenuates pulmonary hypertension in mice.* J Exp Med, 2018. **215**(8): p. 2175-2195.

22.   Lambrecht, B.N. and H. Hammad, *The immunology of asthma.* Nat Immunol, 2015. **16**(1): p. 45-56.

23.   Teach, S.J., et al., *Seasonal risk factors for asthma exacerbations among inner-city children.* J Allergy Clin Immunol, 2015. **135**(6): p. 1465-73 e5.

24.   Jaramillo, R., et al., *Relation between objective measures of atopy and myocardial infarction in the United States.* J Allergy Clin Immunol, 2013. **131**(2): p. 405-11 e1-11.

25.   Andersson, C.K., et al., *Novel site-specific mast cell subpopulations in the human lung.* Thorax, 2009. **64**(4): p. 297-305.

26.   Dahlin, J.S. and J. Hallgren, *Mast cell progenitors: origin, development and migration to tissues.* Mol Immunol, 2015. **63**(1): p. 9-17.

27.   Chaouat, A., et al., *Role for interleukin-6 in COPD-related pulmonary hypertension.* Chest, 2009. **136**(3): p. 678-687.

28.   Prins, K.W., et al., *Interleukin-6 is independently associated with right ventricular function in pulmonary arterial hypertension.* J Heart Lung Transplant, 2018. **37**(3): p. 376-384.

29.   Breitling, S., et al., *The mast cell-B cell axis in lung vascular remodeling and pulmonary hypertension.* Am J Physiol Lung Cell Mol Physiol, 2017. **312**(5): p. L710-L721.

30.   Cho, W.K., et al., *IL-13 receptor alpha2-arginase 2 pathway mediates IL-13-induced pulmonary hypertension.* Am J Physiol Lung Cell Mol Physiol, 2013. **304**(2): p. L112-24.

31.   Takagi, K., et al., *IL-13 enhances mesenchymal transition of pulmonary artery endothelial cells via down-regulation of miR-424/503 in vitro.* Cell Signal, 2018. **42**: p. 270-280.

32.   Platzer, B., M. Stout, and E. Fiebiger, *Functions of dendritic-cell-bound IgE in allergy.* Mol Immunol, 2015. **68**(2 Pt A): p. 116-9.

33.   Perros, F., et al., *Dendritic cell recruitment in lesions of human and experimental pulmonary hypertension.* Eur Respir J, 2007. **29**(3): p. 462-8.

34.   Baravalle, G., et al., *Antigen-conjugated human IgE induces antigen-specific T cell tolerance in a humanized mouse model.* J Immunol, 2014. **192**(7): p. 3280-8.

35.   Sallmann, E., et al., *High-affinity IgE receptors on dendritic cells exacerbate Th2-dependent inflammation.* J Immunol, 2011. **187**(1): p. 164-71.

36.   Farha, S., et al., *Mast cell number, phenotype, and function in human pulmonary arterial hypertension.* Pulm Circ, 2012. **2**(2): p. 220-8.
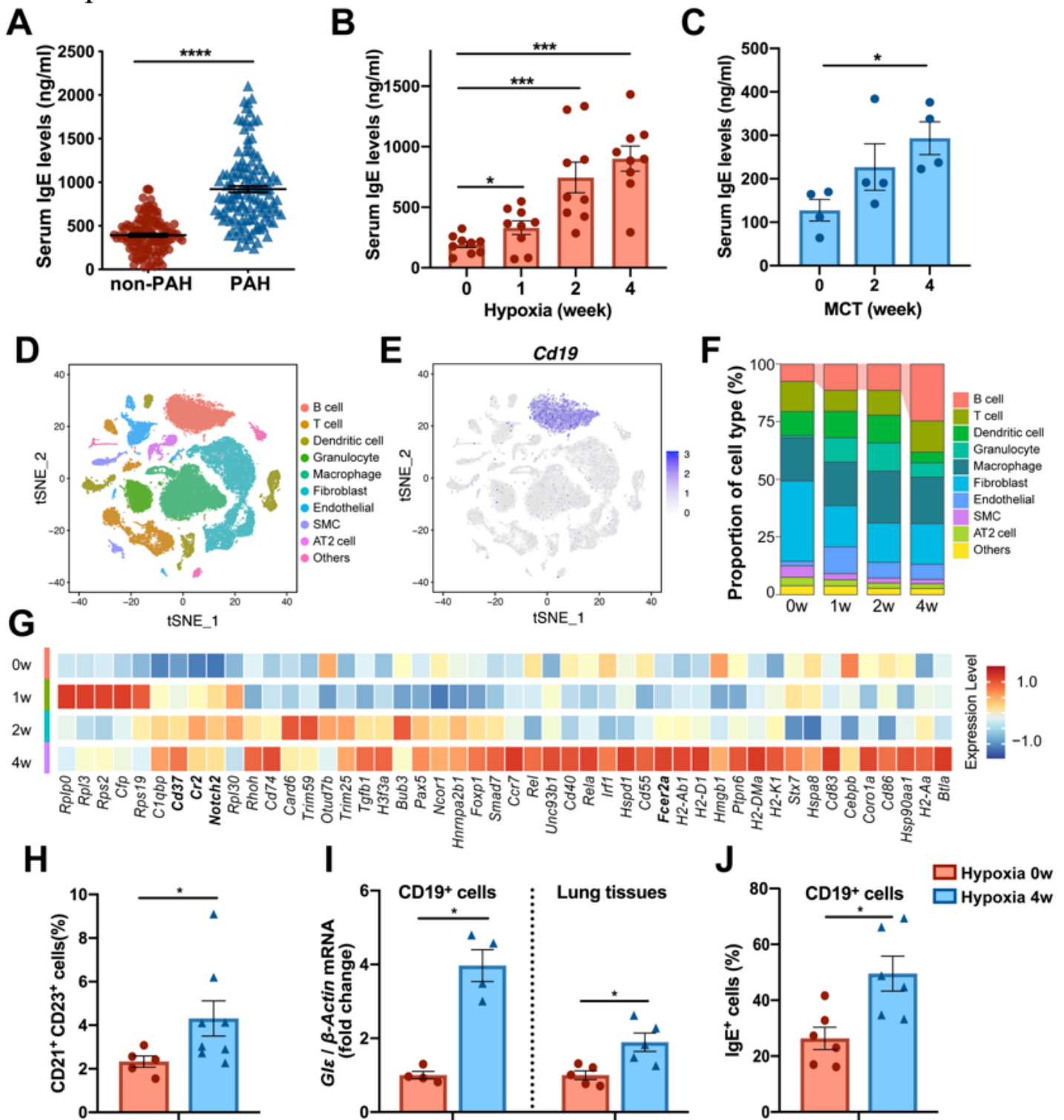
Figures

Figure 1

Serum IgE levels in PAH patients and PH animal models. A. Serum IgE levels of IPAH/HPAH patients and sex-age-matched healthy controls. (non-PAH, n=116; IPAH/HPAH, n=124). B. Serum IgE levels in mice with hypoxia-induced PH (n=9). C. Serum IgE levels in rat with MCT-induced PH (n=4). D. t-Stochastic Neighbor Embedding (t-SNE) representation of aligned gene expression data of cells extracted from lung tissues of four hypoxic groups, showing the partition of distinct clusters. E. The expression of B cell marker gene

Cd19 exhibited on t-SNE plot (gene expression log-normalized by Seurat). F. The percentage of B cells among total cells from the four hypoxic groups. G. Heatmap of key genes differentially expressed during hypoxia exposure. H. Flow cytometry quantification of CD21+CD23+ B cells (0w, n=5; 4w, n=8). I. Relative expression of Glε mRNA in CD19+ B cells (n=4) and lung tissues (n=5). J. Flow cytometry quantification of IgE+ cells in CD19+ cells (n=6). For A, H-J, data are shown as mean ± SEM and the differences between groups were evaluated by unpaired two-tailed t-test. For B and C, data are shown as mean ± SEM and the differences between groups were assessed by one-way ANOVA with LSD-t test. *p<0.05, **p<0.01, ***p<0.001.
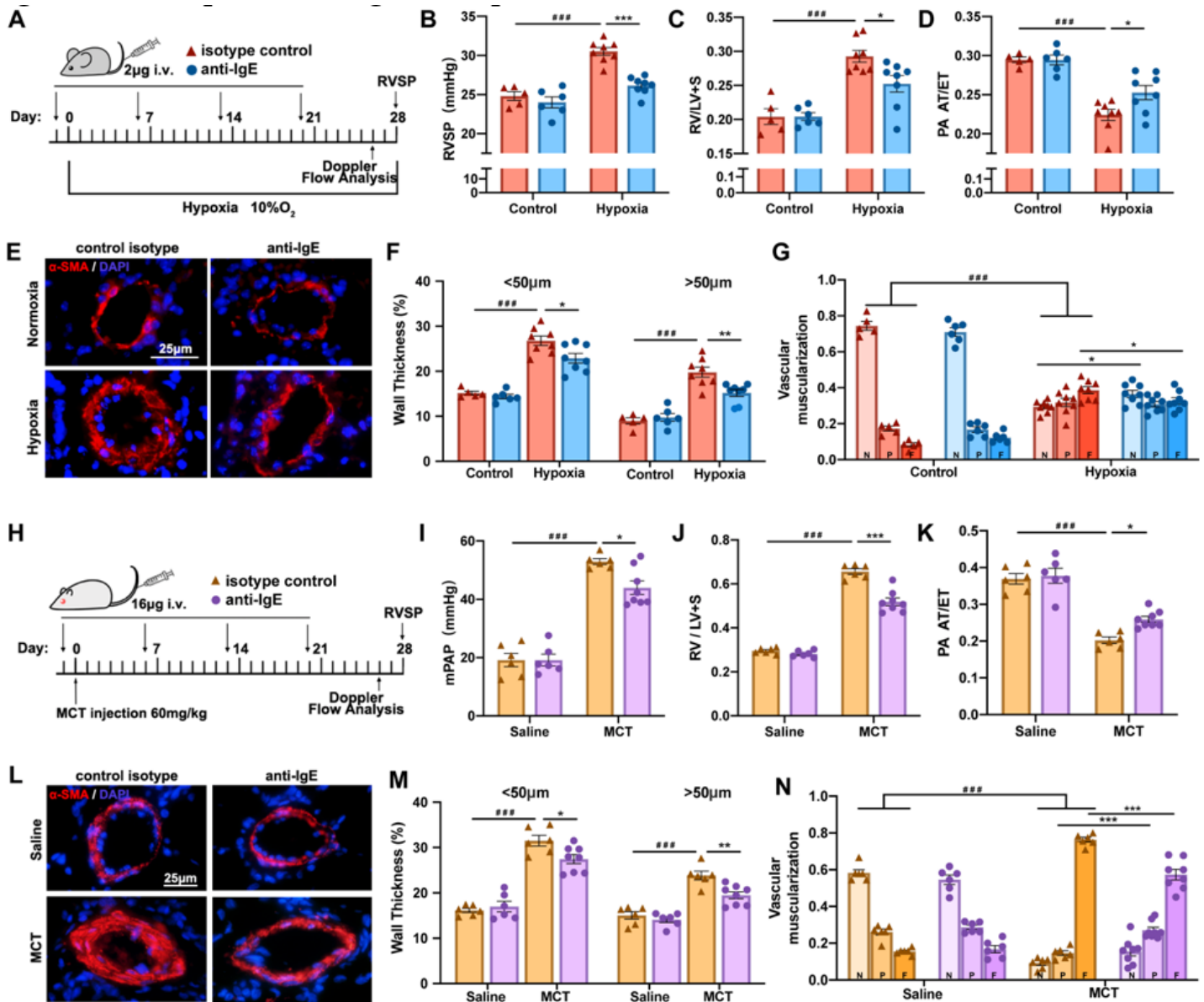

Figure 2

Blocking serum IgE attenuated the development experimental PH in mice and rats. A. Schematic diagram of a preventative study testing the blockade of IgE by neutralizing antibody in the mouse model of hypoxia-induced PH (i.v. indicates tail vein injection; normoxia: n=5 mice were injected with isotype control antibody and n=6 with anti-IgE; hypoxia: n=8 for each group). B. RVSP of isotype control and anti-

IgE treated mice under normoxia or hypoxia. C. RV/LV+S of the different experimental groups. D. PA AT/ET of the different experimental groups. E. Representative images of α-SMA immunofluorescent staining. Scale bar=25μm. F. Quantification of wall thickness of the pulmonary vasculature (pulmonary vascular medial thickness to total vessel size), for vessels of 20-50μm and 50-100μm in diameter, respectively. G. Proportion of non-muscularized (N), partially muscularized (P), or full muscularized (F) pulmonary vessels of 20-100μm in diameter. H. Schematic diagram of a preventative study testing the blockade of IgE by neutralizing antibody in rats with MCT-induced PH (i.v. indicates tail vein injection; Saline: n=6 rats for each group; MCT: n=6 rats were injected with isotype control antibody and n=8 with anti-IgE). I. mPAP of rats from the different experimental groups. J. RV/LV+S of rats from the different experimental groups. K. PA AT/ET of rats from the different experimental groups. L. Representative images of α-SMA immunofluorescent staining. Scale bar=25μm. M. Quantification of wall thickness. N. Proportion of non-muscularized (N), partially muscularized (P), or full muscularized (F) pulmonary vessels of 20-100μm in diameter from indicated rats. All above results of quantitative analysis are shown as mean ± SEM, and differences between multiple groups were evaluated by two-way ANOVA with Bonferroni's post hoc test. $*p<0.05$, $**p<0.01$, and $***p<0.001$ for anti-IgE versus isotype control-treated animals with hypoxia- or MCT-induced PH, $###p<0.001$ for isotype control-treated animals hypoxia vs. normoxia or Saline vs. MCT groups.
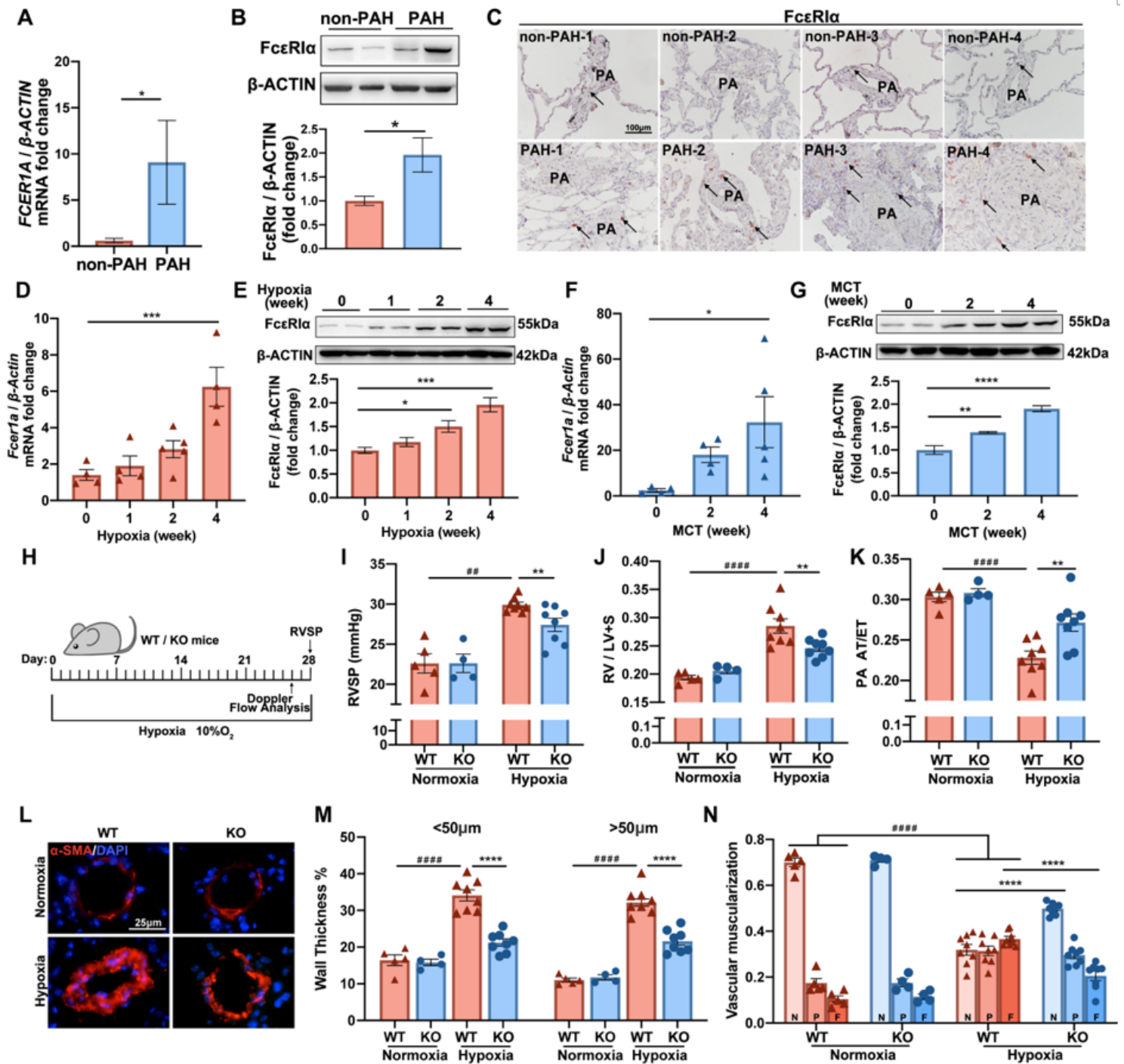
Figure 3

Fcer1a deficiency attenuated hypoxia-induced PH in mice. A. Relative FCER1A mRNA expression in the lung tissues of control subjects (non-PAH) and PAH patients. B. Representative western blot (top) and quantification of FcεRIα and β-ACTIN (bottom) in the lung tissues from control subjects (non-PAH) and PAH patients (n=4 each). C. Representative images of FcεRIα immunohistochemical staining of the lung sections from control subjects (non-PAH) and PAH patients. Scale bar=100μm. D. Relative Fcer1a mRNA expression in lung tissues of mice with hypoxia-induced PH (0w, n=4; 1w, n=4; 2w, n=5; 4w, n=4). E. Representative western blot (top) and quantification of FcεRIα relative to β-ACTIN (bottom) in the lung

tissues of mice with hypoxia-induced PH (n=4 for each group). F. Relative Fcer1a mRNA expression in the lung tissue of rats with MCT-induced PH (0w, n=4; 2w, n=4; 4w, n=5). G. Representative western blot (top) and quantification of FcεRIα and β-ACTIN (bottom) in lung tissue of rats with MCT-induced PH (n=4 for each group). H. Schematic diagram for an experiment testing in Fcer1a+/+ (WT) and Fcer1a-/- (KO) mice in hypoxia-induced PH (normoxia: n=5 for WT and n=4 for KO; hypoxia: n=8 for each group). I. RVSP of WT and KO mice under normoxia and hypoxia. J. RV/LV+S of WT and KO mice under normoxia and hypoxia. K. PA AT/ET of WT and KO mice under normoxia and hypoxia. L. Representative images of α-SMA immunofluorescent staining of the lung sections from WT and KO mice under hypoxia. Scale bar=25µm. M. Quantification of the percentage of wall thickness, classified into 20-50µm and 50-100µm in diameter. N. Proportion of non-muscularized (N), partially muscularized (P), or full muscularized (F) pulmonary vessels (20-100µm in diameter). For A and B, quantitative results are shown as mean ± SEM and differences between groups were assessed by unpaired two-tailed t-test. For D-G, quantitative results are shown as mean ± SEM and multi-group comparison was performed using one-way ANOVA with LSD-t test. For I-K, M, N, quantitative results are shown as mean ± SEM with multi-group comparison by two-way ANOVA with Bonferroni's post hoc test. $*p<0.05$, $**p<0.01$, $***p<0.001$ and $****p<0.0001$ hypoxic WT vs. hypoxic KO, $\#\#p<0.01$, $\#\#\#p<0.001$ and $\#\#\#\#p<0.0001$ normoxic WT vs. hypoxic WT.
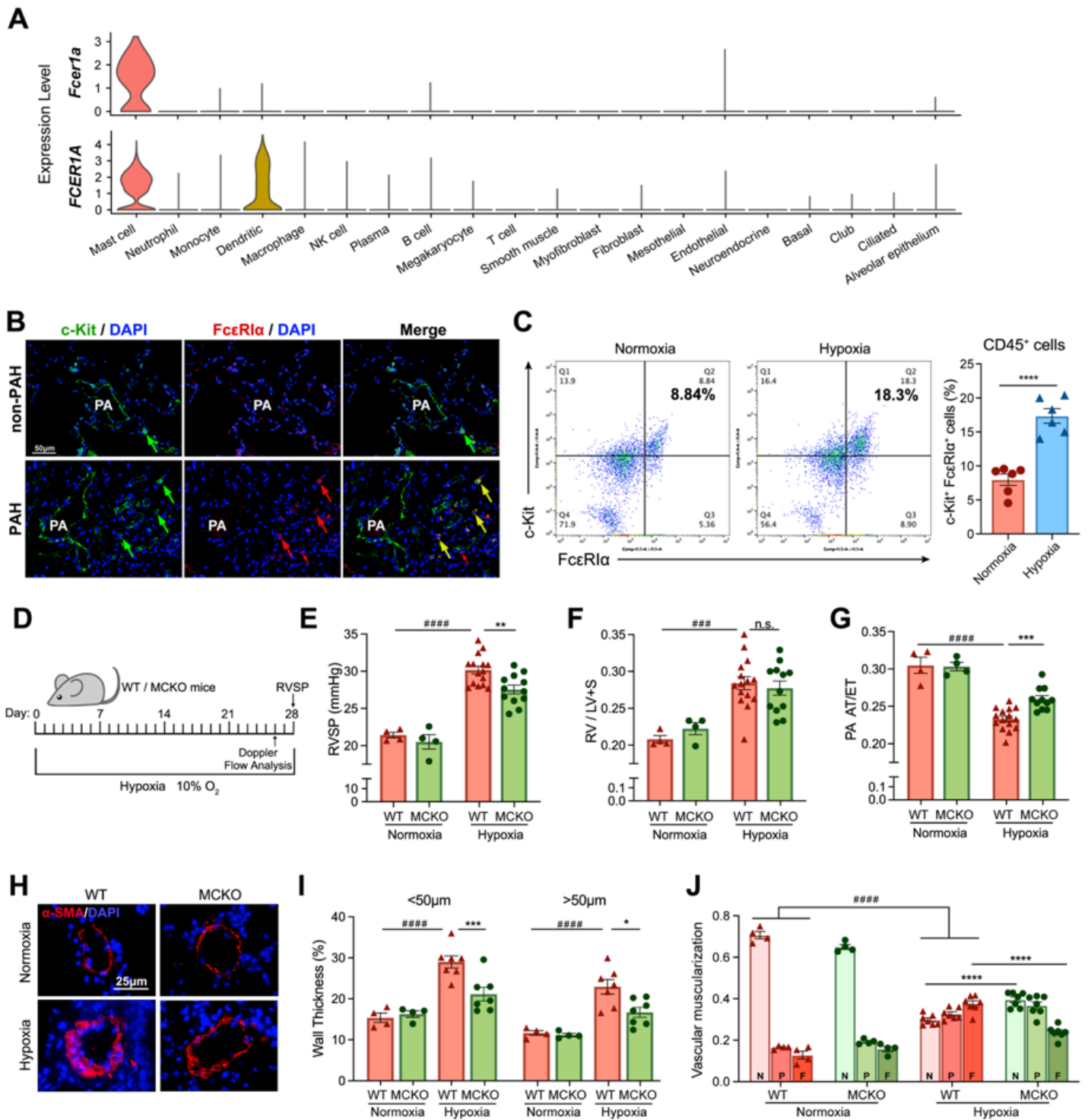
Figure 4

FcεRIα expression in mast cells contributed to the development of PH in a mouse model. A. Violin plots of the expression of Fcer1a in mouse lung tissues(top) and FCER1A in human lung tissues(bottom). B. Representative images showing staining of c-Kit and FcεRIα in lung sections of control subjects (non-PAH) and PAH patients. The arrows indicate examples of staining positive cells. Scale bar=50μm. C. Representative flow cytometric analysis of c-Kit+ FcεRIα+ cells among CD45+cells in lung tissues of mice under normoxia and hypoxia. The percentage of c-Kit+ FcεRIα+ cells among CD45+ cells in lung tissues

of mice under normoxia and hypoxia (n=6 per group). D. Schematic diagram of an experiment testing Fcer1aflox/flox (WT) and Fcer1aMC-/- (MCKO) mice in hypoxia-induced PH (normoxia: n=4; hypoxia: n=15 for WT group and n=12 for MCKO group). E. RVSP of WT and MCKO mice under normoxia and hypoxia. F. RV/LV+S of these mice. G. PA AT/ET of these mice. H. Representative images of α-SMA immunofluorescent staining of the lung sections. Scale bar=25μm. I. Quantification of wall thickness of pulmonary vessels, 20-50μm and 50-100μm in diameter. J. Proportion of non-muscularized (N), partially muscularized (P), or full muscularized (F) pulmonary vessels of 20-100μm in diameter from indicated mice (normoxia: n=4; hypoxia: n=7). All above quantitative results are shown as mean ± SEM, and differences between multiple groups were evaluated by two-way ANOVA with Bonferroni's post hoc test. *p<0.05, **p<0.01, ***p<0.001 and ****p<0.0001 for hypoxic MCKO vs. hypoxic WT, ###p<0.001 and ####p<0.0001 for normoxic WT vs. hypoxic WT, and n.s. indicates no significant difference.
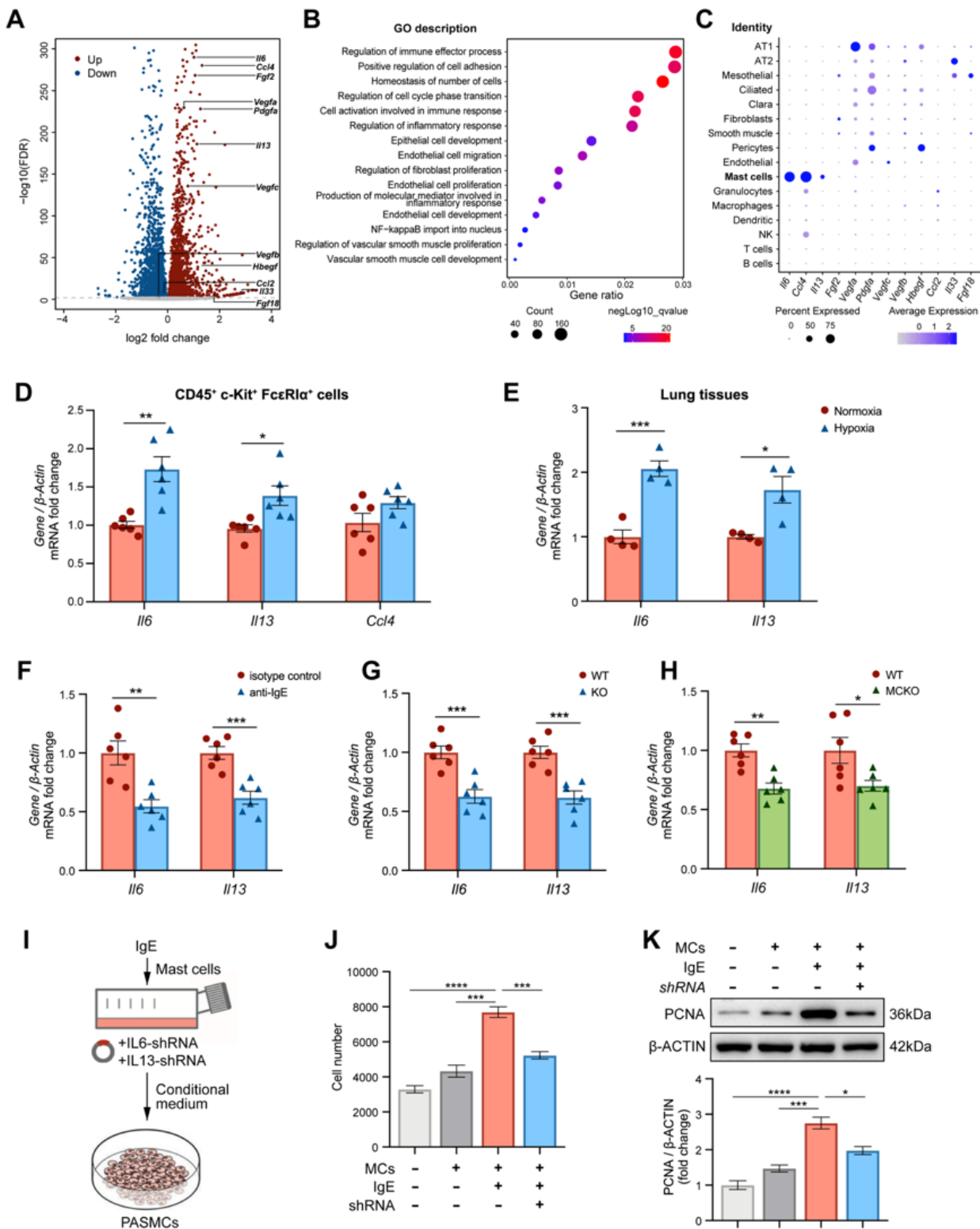
Figure 5

IgE stimulated MCs to produce IL6 and IL13 in experimental PH. A. Volcano plot of differentially expressed genes between BMMCs treated with and without IgE, with two samples for each group; P value was adjusted by false discovery rate (FDR). B. Bubble plot of GO pathway enrichment of the differentially expressed genes in response to IgE. C. Dot plot of gene expression in cell clusters. D. Relative mRNA expression of Il6, 1I13 and Ccl4 in sorted CD45+ c-Kit+ FcεRIα+ cells from lung tissues of mice under

normoxia and hypoxia. E. Relative mRNA expression of Il6 and Il13 in lung tissues from mice under normoxia and hypoxia. F. Relative mRNA expression of Il6 and Il13 in lung tissues from hypoxic mice injected with IgE-neutralizing antibody or isotype control. G. Relative mRNA expression of Il6 and Il13 in lung tissues from WT or KO mice after hypoxia exposure. H. Relative mRNA expression of Il6 and Il13 in lung tissues from WT or MCKO mice after hypoxia exposure. I. Schematic diagram of the MC and PASMC co-culture experiment. J. Quantification of cell number of PASMCs co-cultured with supernatant from IgE-treated MCs transfected with or without shIL6 and shIL13 measured by CCK8 assay. K. Representative western blots and quantification of PCNA (proliferating cell nuclear antigen) in the PASMCs. All values are presented as the mean ± SEM. For D, n=6; E, n=4; F-H, n=6 for each group, and differences were evaluated by unpaired two-tailed t-test. For J and K, n=3 for each group, and differences were evaluated by one-way ANOVA with LSD-t test. $*p < 0.05$, $**p < 0.01$, and $***p < 0.001$.
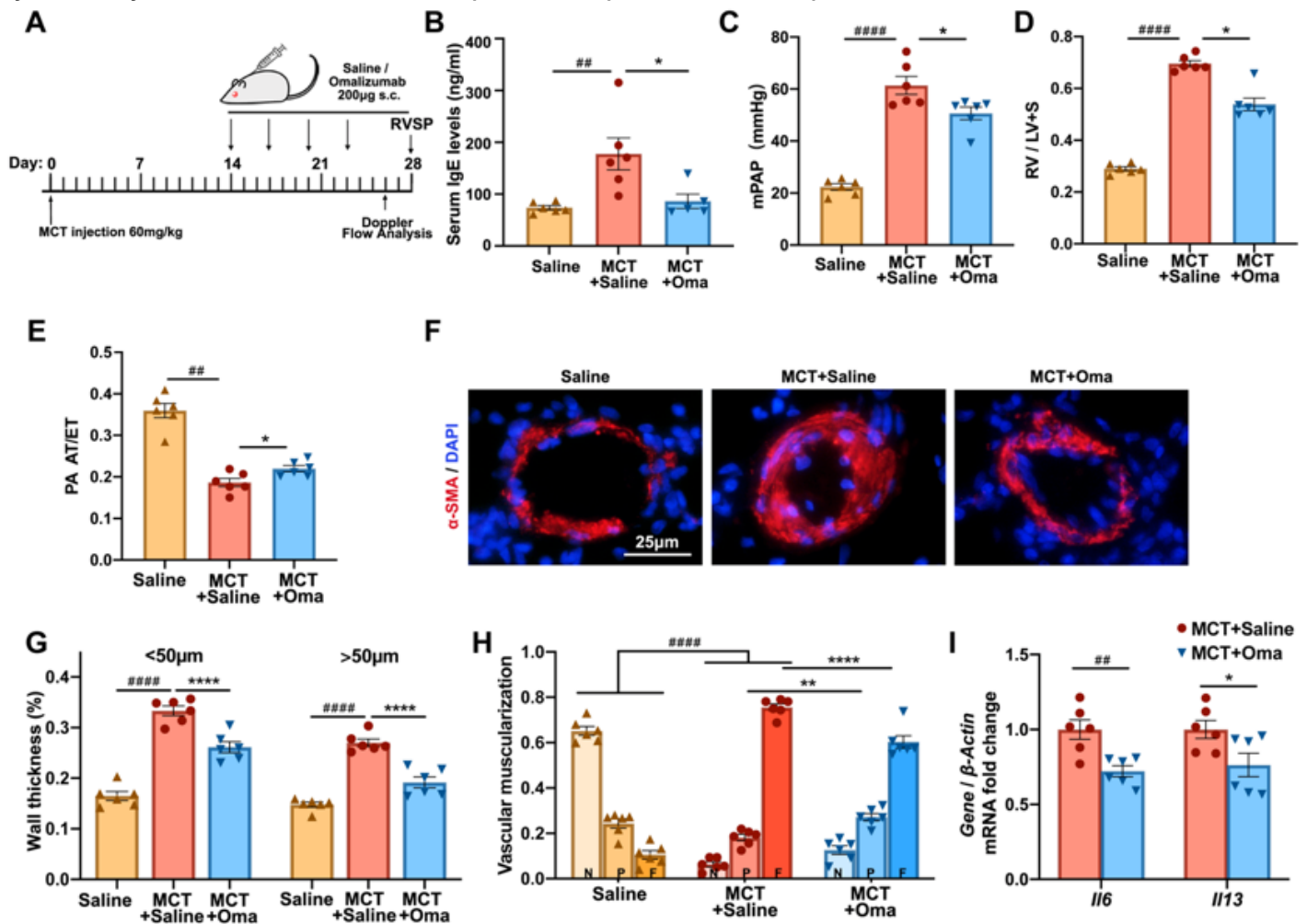

Figure 6

Anti-IgE therapy using omalizumab might prevent established PH development in MCT rats. A. Schematic diagram of anti-IgE therapy on MCT-induced rats PH model using Omalizumab. The treatment of Omalizumab (200µg, s.c.) was started from 14 days post-MCT injection (n=6 for each group). B. Serum IgE levels in Saline or Omalizumab (Oma) treated MCT rats. C. mPAP of indicated rats. D. RV/LV+S of indicated rats. E. PA AT/ET of indicated rats. F. Representative images of α-SMA immunofluorescence

staining of the lung sections from rats in MCT+Saline group and MCT+Oma group. Scale bar=25µm. G. Quantification of wall thickness of pulmonary vasculature, 20-50µm and 50-100µm in diameter. H. Proportion of non-muscularized (N), partially muscularized (P), or full muscularized (F) pulmonary vasculatures of 20-100µm in diameter from indicated rats. I. Relative Il6 and Il13 mRNA expression in lung tissues from indicated rats. All above quantitative analysis results are shown as mean ± SEM. For B-E, G and H, difference between multiple groups was evaluated by One-way ANOVA with LSD-t test. For I, difference between groups was evaluated as mean ± SEM by unpaired two-tailed t-test. *p<0.05, **p<0.01 and ****p<0.0001 MCT+Saline group vs. MCT+Oma group, ##p<0.01 and ###p<0.001 Saline group vs. MCT+Saline group.

Supplementary Files

This is a list of supplementary files associated with this preprint. Click to download.

- NCVRsup.docx